

Valley density-wave and multiband superconductivity in Fe-pnictides

Vladimir Cvetkovic¹ and Zlatko Tesanovic¹

¹*Department of Physics & Astronomy, The Johns Hopkins University, Baltimore, MD 21218*

(Dated: October 15, 2008)

The key feature of the Fe-based superconductors is their quasi 2D multiband Fermi surface (FS). By relating the problem to a negative U Hubbard model and its superconducting ground state, we show that the defining instability of such a FS is the valley density-wave (VDW), a *combined* spin/charge density-wave at the wavevector connecting the electron and hole valleys. As the valley parameters change by doping or pressure, the fictitious superconductor experiences “Zeeman splitting”, eventually going into a non-uniform “Fulde-Ferrell-Larkin-Ovchinnikov” (FFLO) state, an *intrinsic* and often *incommensurate* VDW of the real world, characterized by the metallic conductivity from the ungapped remnants of the FS. When “Zeeman splitting” exceeds the “Chandrasekhar-Clogston” limit, the “FFLO” state disappears, and the VDW is destabilized. Near this point, the VDW fluctuations are an essential ingredient of high- T_c superconductivity in Fe-pnictides.

Recently, the superconductivity below 7 K in LaOFeP [1] led to the discovery of high $T_c \sim 26$ K in its doped sibling LaO_{1-x}F_xFeAs ($x > 0.1$) [2]. Even higher T_c 's were found by replacing La with other rare-earths (RE), up to the current record of $T_c = 55$ K [3]. These are the first non-cuprate superconductors exhibiting such high T_c 's and their discovery has touched off a storm of activity.

In this paper, we introduce a new element into the theoretical debate by considering a unified model of spin-density wave, structural deformation and superconductivity in Fe-pnictides. The model is simple but it contains the necessary physical features. The essential ingredient are electron and hole pockets (valleys) of the quasi two-dimensional (2D) multiply-connected Fermi surface (FS) [4–6]. To extract the basic physics we consider spinless electrons first, and only a single electron and a single hole band with identical band parameters. We then show that this model can be related to a 2D *negative* U Hubbard model, the ground state of which is known exactly – it is a superconductor [7]. In real FeAs materials, this fictitious superconductivity translates into a valley density-wave (VDW), a unified state representing a combination of spin, charge and orbital density-waves (SDW/CDW/ODW) at the *commensurate* wavevector \mathbf{M} connecting the two valleys. Next, we introduce two different “chemical potentials”, $\mu^e \neq \mu^h$ for the electron and the hole valleys – this corresponds to the external Zeeman splitting in our fictitious negative U Hubbard model. As $\delta\mu = \mu^e - \mu^h$ increases, so does this Zeeman splitting, and eventually our fictitious superconducting state approaches to and exceeds the “Chandrasekhar-Clogston” limit, giving way to a *non-uniform* Fulde-Ferrell-Larkin-Ovchinnikov (FFLO) ground state at an *incommensurate* wavevector \mathbf{q} , where $|\mathbf{q}|$ is set by $\delta k_F = k_F^e - k_F^h$, and thus by doping x . This “FFLO state” is nothing but an incommensurate (IC) VDW at the wavevector $\mathbf{M} + \mathbf{q}$. Finally, as $\delta k_F(x)$ exceeds certain critical value $\delta k_c(x_c)$, the “superconducting” state is completely destroyed and so is the VDW in a true material. However, for δk_F above but near δk_c , we consider strong “superconducting” fluc-

tuations and find that these VDW fluctuations can induce *real* superconductivity in Fe-pnictides (see Fig. 1).

The band structure of Fe-pnictides [4–6] can be parametrized by the five-orbital tight-binding model [8, 9]. The key feature is the *multiband* nature of the FS, possessing both hole and electron sections. The basic physics is captured by the Hamiltonian describing two hole (c^β) and two electron (d^α) bands centered at the Γ and M points of the 2D Brillouin zone (BZ), respectively,

$$H = H_0 + H_{int}, \quad (1)$$

$$H_0 = \sum_{\mathbf{k}, \sigma, \alpha} \epsilon_{\mathbf{k}}^{(\alpha)} d_{\mathbf{k}, \sigma}^{(\alpha)\dagger} d_{\mathbf{k}, \sigma}^{(\alpha)} + \sum_{\mathbf{k}, \sigma, \beta} \epsilon_{\mathbf{k}}^{(\beta)} c_{\mathbf{k}, \sigma}^{(\beta)\dagger} c_{\mathbf{k}, \sigma}^{(\beta)}, \quad (2)$$

$$H_{int} = \frac{1}{2} \int d^2\mathbf{r} d^2\mathbf{r}' V(\mathbf{r}, \mathbf{r}') n(\mathbf{r}) n(\mathbf{r}'), \quad (3)$$

where $\sigma, \sigma' = \uparrow, \downarrow$ and $\alpha, \beta = 1, 2$ are the spin and band labels, respectively, $\epsilon_{\mathbf{k}}^{(\alpha, \beta)}$ is the electron (hole) dispersion near the FS, $V(\mathbf{r}, \mathbf{r}')$ is the effective interaction and $n(\mathbf{r}) = \sum_{\sigma} \psi_{\sigma}^{\dagger}(\mathbf{r}) \psi_{\sigma}(\mathbf{r})$, with $\psi_{\sigma}(\mathbf{r}) = \sum_{\mathbf{k}, \alpha} d_{\mathbf{k}, \sigma}^{(\alpha)} \varphi_{\mathbf{k}}^{(\alpha)}(\mathbf{r}) + \sum_{\mathbf{k}, \beta} c_{\mathbf{k}, \sigma}^{(\beta)} \phi_{\mathbf{k}}^{(\beta)}(\mathbf{r})$. $\varphi_{\mathbf{k}}^{(\alpha)}(\mathbf{r})$ and $\phi_{\mathbf{k}}^{(\beta)}(\mathbf{r})$ are the Bloch wavefunctions of electron (hole) bands. For simplicity, (3) includes only the screened density-density repulsion; its form becomes more complex if we integrate out the bands away from the Fermi level E_F , generating additional interactions in the spin and interband (orbital) channels. We further simplify the problem by exploiting the fact that all electron (hole) bands have E_F near their bottom (top) and their Fermi wavevectors k_F 's are $\ll M$. This allows us to restrict our attention to the first BZ and take continuum limit, with $V(\mathbf{r}, \mathbf{r}') \rightarrow V(\mathbf{r} - \mathbf{r}')$.

H_{int} (3) generates three classes of vertices: i) the intraband ($d^\dagger d d^\dagger d$ and $c^\dagger c c^\dagger c$), ii) the interband ($d^\dagger d c^\dagger c$), and iii) the mixed ($d^\dagger c c^\dagger d$ + h.c. and $c^\dagger d c^\dagger d$ + h.c.). All arise from $H_{int} \rightarrow \frac{1}{2} \sum_{\mathbf{q}} \tilde{V}_{\mathbf{q}} n_{\mathbf{q}} n_{-\mathbf{q}}$, where

$$n_{\mathbf{q}} = \sum_{\mathbf{k} \sigma \alpha \alpha'} \zeta_{\mathbf{k}+\mathbf{q}, \mathbf{k}}^{(\alpha \alpha')} d_{\mathbf{k}+\mathbf{q}, \sigma}^{(\alpha)\dagger} d_{\mathbf{k}, \sigma}^{(\alpha')} + \sum_{\mathbf{k} \sigma \beta \beta'} \zeta_{\mathbf{k}+\mathbf{q}, \mathbf{k}}^{(\beta \beta')} c_{\mathbf{k}+\mathbf{q}, \sigma}^{(\beta)\dagger} c_{\mathbf{k}, \sigma}^{(\beta')} + \sum_{\mathbf{k} \sigma \alpha \beta} \gamma_{\mathbf{k}+\mathbf{q}, \mathbf{k}}^{(\alpha \beta)} d_{\mathbf{k}+\mathbf{q}, \sigma}^{(\alpha)\dagger} c_{\mathbf{k}, \sigma}^{(\beta)} + \text{h.c.} \quad (4)$$

and $\tilde{V}_{\mathbf{q}}$ is the Fourier transform (FT) of $V(\mathbf{r} - \mathbf{r}')$. In addition, $\zeta_{\mathbf{k},\mathbf{k}'}^{(\alpha\alpha')} = \int d^2\mathbf{r} e^{i(\mathbf{k}'-\mathbf{k})\cdot\mathbf{r}} \varphi_{\mathbf{k}}^{(\alpha)*}(\mathbf{r}) \varphi_{\mathbf{k}'}^{(\alpha')}(\mathbf{r})$, $\zeta_{\mathbf{k},\mathbf{k}'}^{(\beta\beta')} = \int d^2\mathbf{r} e^{i(\mathbf{k}'-\mathbf{k})\cdot\mathbf{r}} \phi_{\mathbf{k}}^{(\beta)*}(\mathbf{r}) \phi_{\mathbf{k}'}^{(\beta')}(\mathbf{r})$, $\gamma_{\mathbf{k},\mathbf{k}'}^{(\alpha\beta)} = \int d^2\mathbf{r} e^{i(\mathbf{k}'-\mathbf{k})\cdot\mathbf{r}} \varphi_{\mathbf{k}}^{(\alpha)*}(\mathbf{r}) \phi_{\mathbf{k}'}^{(\beta)}(\mathbf{r})$. Generically, the intra and the interband vertices are comparable in magnitude while the mixed ones are smaller.

We now observe that the shapes of different sections of the FS (Fig. 1) resemble each other to a reasonable degree. Furthermore, various masses are also roughly similar [8, 9]. Thus, to make theoretical progress, it is useful to first assume that all electron and hole bands are equal $\epsilon_{\mathbf{k}}^{(\alpha=1)} = \epsilon_{\mathbf{k}}^{(\alpha=2)} = -\epsilon_{\mathbf{k}}^{(\beta=1)} = -\epsilon_{\mathbf{k}}^{(\beta=2)}$. After making the particle-hole (p-h) transformation $d_{\mathbf{k},\sigma}^{(\alpha)} \rightarrow e_{\mathbf{k},\sigma}^{(\alpha)}$, $c_{\mathbf{k},\sigma}^{(\alpha)} \rightarrow \sigma h_{\mathbf{k},-\sigma}^{(\alpha)\dagger}$, the Hamiltonian (1) becomes:

$$H_{\text{SU}(8)} \rightarrow \sum_{\mathbf{k},\sigma,\mu} \epsilon_{\mathbf{k}} \Psi_{\mathbf{k},\sigma}^{(\mu)\dagger} \Psi_{\mathbf{k},\sigma}^{(\mu)} + H'_{\text{int}}, \quad (5)$$

where $\Psi^{(\mu)\dagger} = (e_1^\dagger, e_2^\dagger, h_1^\dagger, h_2^\dagger)$. Ignoring the effects of bands away from the FS, the kinetic part of $H_{\text{SU}(8)}$ (5) has an exact $\text{SU}(8)$ symmetry involving orbital (*both* electron and hole) and spin degrees of freedom, μ and σ , respectively. This symmetry can be used to classify various vertices in H'_{int} – ultimately generated by H_{int} (3) which itself has only $\text{U}(1)_{\text{charge}} \times \text{SU}(2)_{\text{spin}}$ symmetry – and analyze various symmetry-breaking patterns, starting with $\text{SU}(8) \rightarrow \text{SU}(4) \times \text{SU}(4)$, as discussed in [10].

To illustrate the physics, we focus here on the *minimal* model: $\text{SU}(8) \rightarrow \text{SU}(2)$. This leaves one with two fermion flavors, e and h . Note that *spin* $\text{SU}(2)$ symmetry is suppressed, but the *orbital* electron-hole symmetry remains, as it is essential for this problem. We now obtain:

$$H_{\text{SU}(2)} = \sum_{\mathbf{k}} \epsilon_{\mathbf{k}} [e_{\mathbf{k}}^\dagger e_{\mathbf{k}} + h_{\mathbf{k}}^\dagger h_{\mathbf{k}}] + \frac{1}{2} \int d^2\mathbf{r} d^2\mathbf{r}' \times \\ [U^e(\mathbf{r} - \mathbf{r}') n^e(\mathbf{r}) n^e(\mathbf{r}') + U^h(\mathbf{r} - \mathbf{r}') n^h(\mathbf{r}) n^h(\mathbf{r}') \\ + 2W(\mathbf{r} - \mathbf{r}') n^e(\mathbf{r}) n^h(\mathbf{r}')] + H_{\text{SU}(2)}^{\text{mixed}}, \quad (6)$$

where $U^{e/h}(\mathbf{r})$ and $W(\mathbf{r})$ are the FTs of $\tilde{V}_{\mathbf{k}-\mathbf{k}'} \langle \zeta_{\mathbf{k},\mathbf{k}'}^{(e/h)} \zeta_{\mathbf{k}',\mathbf{k}}^{(e/h)} \rangle_{\text{FS}}$ and $-\tilde{V}_{\mathbf{k}-\mathbf{k}'} \langle \zeta_{\mathbf{k},\mathbf{k}'}^{(e)} \zeta_{\mathbf{k}',\mathbf{k}}^{(h)} \rangle_{\text{FS}}$, respectively. $\langle \dots \rangle_{\text{FS}}$ indicates the \mathbf{k} - and \mathbf{k}' -dependence was replaced by the FS average – this is justified later. The $\text{SU}(2)$ symmetry implies $U^e(\mathbf{r}) = U^h(\mathbf{r})$. Finally, $H_{\text{SU}(2)}^{\text{mixed}}$ contains smaller mixed vertices and we initially – but only temporarily – set it to zero, $H_{\text{SU}(2)}^{\text{mixed}} \rightarrow 0$.

$W(\mathbf{r})$ in $H_{\text{SU}(2)}$ (6) has the sign *opposite* to $V(\mathbf{r})$. This is the result of the p-h transformation and indicates that, us having started with a (screened) Coulomb repulsion between the original electrons, the e and h flavors now mutually *attract*. Consequently, at low energies, $H_{\text{SU}(2)}$ (without $H_{\text{SU}(2)}^{\text{mixed}}$) is *equivalent* to the *negative* U Hubbard model at low (or high) x , assuming that $W(\mathbf{r})$ is short-ranged and $\epsilon_{\mathbf{k}}$ can be represented in the effective mass

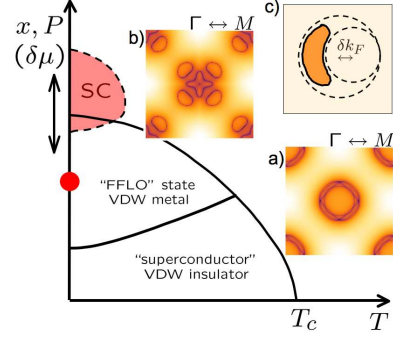


FIG. 1: Phase diagram of Fe-pnictides, depicting the evolution of our fictitious superconductor from the fully gapped VDW insulator to the “FFLO superconductor” – a partially gapped metallic VDW – to the *real* superconductor (SC) under the influence of the “Zeeman splitting” $\delta\mu$ (doping or pressure). Red dot symbolizes the known FeAs parent compounds and the regime below it might be physically inaccessible. Insets: FS of a) the normal state in the folded ($\Gamma \leftrightarrow M$) BZ [9], b) the VDW metal (computed with the interband interaction set to unity) – this is the C_{4v} version of c) the continuum FFLO state [11]. The remaining states are fully gapped.

approximation ($W(\mathbf{r}) \rightarrow W\delta(\mathbf{r})$ and $\epsilon_{\mathbf{k}} \rightarrow \mathbf{k}^2/2m$). Both assumptions should be valid since $k_F \ll M$. The ground state is a “superconductor”, with an anomalous correlator $\langle e^\dagger h^\dagger \rangle \neq 0$, where $e^\dagger (h^\dagger)$ creates a “spin up (down)” fermion $f_\uparrow (f_\downarrow)$. For $T > T_c \sim E_F \exp(-1/N(0)W)$, the system is in its normal state (see phase diagram in Fig. 1). At $T < T_c$ one enters a broken symmetry state, with “off-diagonal” long range order and gapped fermions.

What is this “superconductivity” in the real world? Retracing our steps, the “off-diagonal” order in $\langle f_{\mathbf{k}\uparrow}^\dagger f_{-\mathbf{k}\downarrow}^\dagger \rangle = \langle e_{\mathbf{k}}^\dagger h_{-\mathbf{k}}^\dagger \rangle$ translates into the diagonal density-wave, $\langle d_{\mathbf{k}}^\dagger c_{\mathbf{k}-\mathbf{M}} \rangle \neq 0$, connecting electrons from two pockets of the FS separated by $\mathbf{M} = (\pi, \pi)$; a *valley* density-wave (VDW). Note that the VDW describes *both* spin *and* charge/orbital density-waves (SDW/CDW/ODW). With the spin $\text{SU}(2)$ symmetry suppressed in our minimal model, one cannot – and *should not* – distinguish between the two. We identify the above VDW (SDW/CDW/ODW combination) with the ordering observed in experiments.

We can pursue this VDW-“superconductor” analogy further: in real FeAs materials, the electron-hole pockets are not identical, the main difference being their distinct k_F ’s. In our fictitious superconductor, this translates to different “chemical potentials”, $\mu^e \neq \mu^h$ for the electron and the hole valleys. This is nothing but the Zeeman splitting in a fictitious negative U Hubbard model. As $\delta\mu = \mu^e - \mu^h$ grows, the “superconducting” state approaches the “Chandrasekhar-Clogston” limit, giving way to a *non-uniform* Fulde-Ferrell-Larkin-Ovchinnikov (FFLO) ground state at an *incommensurate* wavevector \mathbf{q} , set by $\delta k_F = k_F^e - k_F^h$. This “FFLO state” is just an

incommensurate (IC) VDW at the wavevector $\mathbf{M} + \mathbf{q}$. Finally, as $\delta k_F(x)$ exceeds certain critical $\delta k_c(x_c)$, the “superconducting” state is destroyed and so is the VDW (SDW/CDW/ODW) in real FeAs (Fig. 1) [12].

The above “superconductor” analysis dealt with an idealized model but its main conclusions apply to the real Fe-pnictides: i) the dominant instability is the VDW at wavevector \mathbf{M} , a *unified* spatially-modulated state manifested through the *combined* SDW/CDW/ODW and a structural transformation [13], the details of which depend on non-universal features of individual materials; ii) since hole and electron valleys are not identical, the VDW is the p-h analog of a fictitious FFLO state, resulting almost always in portions of the FS which are *not gapped* (Fig. 1). Consequently, the SDW/CDW/ODW’s in FeAs are highly itinerant and coexist with finite density of normal charge carriers, exhibiting metallic conductivity [14]; and, finally, iii) the Hamiltonian $H_{\text{SU}(2)}$ (6) *without* the mixed vertices (i.e., with $H_{\text{SU}(2)}^{\text{mixed}} \rightarrow 0$) contains only *three* basic ground states: fictitious uniform and non-uniform FFLO “superconductor” (C and IC VDW) and the normal state (Fig. 1). *Thus, if purely electronic interactions are to have a prominent role in generating Fe-based superconductivity, this effect must arise from $H_{\text{SU}(2)}^{\text{mixed}}$.*

With this in mind, we now restore $H_{\text{SU}(2)}^{\text{mixed}}$ to address the *real* superconductivity in our “superconductor” model: the mixed vertices are $G_1 d^\dagger c c^\dagger d + \text{h.c.} \leftrightarrow G_1 e^\dagger h^\dagger h e + \text{h.c.}$ and $G_2 c^\dagger d c^\dagger d + \text{h.c.} \leftrightarrow G_2 h e h e + \text{h.c.}$. We assume $G_1, G_2 \ll W, U_h, U_e$, as will be justified momentarily. At the lowest order, the effect of G_1, G_2 is

$$\begin{aligned} g_W(\omega) &= g_W + g_W^2 \ln\left(\frac{\Lambda}{\omega}\right) \\ g_2(\omega) &= g_2 + 2g_2 g_W \ln\left(\frac{\Lambda}{\omega}\right)_c - 2g_2 g_1 \ln\left(\frac{\Lambda}{\omega}\right) + 2g_2 g_W \ln\left(\frac{\Lambda}{\omega}\right)_v \\ g_1(\omega) &= g_1 - g_1^2 \ln\left(\frac{\Lambda}{\omega}\right) - g_2^2 \ln\left(\frac{\Lambda}{\omega}\right) + 2g_1 g_W \ln\left(\frac{\Lambda}{\omega}\right)_v, \end{aligned} \quad (7)$$

$$\zeta_{\mathbf{k}, -\mathbf{k}}^{(\alpha)} = \pm \left(\sum_{\mu \in \text{even}} |b_\mu^{(\alpha)}|^2 - \sum_{\mu \in \text{odd}} |b_\mu^{(\alpha)}|^2 \right), \quad (8)$$

where g_W, g_1 and g_2 are the dimensionless vertices W, G_1 and G_2 , respectively. The logarithmic divergence arises from the perfect nesting of the hole and electron bands (our fictitious “Cooper” instability), while $\ln\left(\frac{\Lambda}{\omega}\right)_{c(v)}$ denotes a crossing (vertex) diagram – it strictly diverges only in the $k_F^{e,h}/M \rightarrow 0$ limit and is otherwise finite.

The first line of (7) is just the mathematical shorthand for our earlier discussion: under renormalization, the coupling constant g_W keeps growing, ultimately generating the VDW instability, driven by W ($-U$ of our fictitious Hubbard model). The last line tells us that G_1 does not interfere; in practice, it can be set to zero. The interesting physics is reserved for G_2 . The growth of g_W fuels the growth of g_2 and thus the mixed vertex describing the resonant pair scattering between the hole and electron bands (the “Josephson” interband vertex $c^\dagger d c^\dagger d + \text{h.c.}$) becomes strongly enhanced as one approaches the VDW (SDW/CDW/ODW) instability. Since $G_2 \ll W$ (see below), g_W always wins, resulting in the VDW order.

The situation changes, however, when the differences between h and e bands are included, i.e., when the “Zeeman splitting” is turned on, by doping or pressure in real FeAs (Fig. 1). This cuts off the “Cooper” divergence, resulting in our “FFLO” state and eventual disappearance of VDW. The remarkable feature of interband pair resonance is that it can produce real superconductivity *irrespective* of its sign [15]. Thus, strongly enhanced G_2 can take advantage of the real-world Cooper singularity – which is always present – and amplify a preexisting *intra-band* superconducting instability or generate one entirely on its own. We will revisit this point near the end.

This is as far as we can go within the idealized picture: we now must face up to the complexities of the real materials. First, there are four, two h and two e , bands which deviate from an ideal parabolic shape and whose k_F ’s are different and, second, all vertices – intra, interband and mixed – have considerable structure as one moves over different portions of the FS. The latter is an important point and reflects a fundamental feature of FeAs: all five d-orbitals need to be included in realistic calculations and various two- and three-orbitals models will fall short in addressing the phenomenology of real materials. Finally, the lattice effects produce modifications to our continuum picture which need to be addressed [12].

We use the full 8+8-band tight-binding model [9] to find the electron ($\varphi_{\mathbf{k}}^{(\alpha)}$) and hole ($\phi_{\mathbf{k}}^{(\beta)}$) wavefunctions. This model yields ζ ’s and γ ’s of Eq. (4) [16]. For a fixed \mathbf{k} , a given ζ varies as \mathbf{k}' goes around the FS. At $\mathbf{k} = \mathbf{k}'$, the normalization of wave-functions sets ζ to 1. As \mathbf{k} and \mathbf{k}' move apart, so does ζ decreases until it reaches its minimum at $\mathbf{k}' = -\mathbf{k}$. Based on the symmetry properties of the atomic orbitals, one obtains ($k_F \ll M$)

where $b_\mu^{(\alpha)}$ is the amplitude of atomic orbital μ in a hole state (α) or, equivalently, an electron state (β). Each orbital’s contribution is determined by its parity (i.e., sign change under $(x, y, z) \rightarrow (-x, -y, z)$); even/odd orbitals contribute with $+/-$, or vice versa. Our model uses orbitals of different parity, and consequently, (8) is bound between -1 and 1 , the precise value depending on the amount of mixing of even and odd orbitals within a state. For example, consider $\zeta^{(h1)}$ and $\zeta^{(h2)}$ [16]. Since both hole bands have a significant contribution of $d_{xz/yz}$ atomic orbitals (odd), both ζ ’s are similarly shaped, sharing the 4-fold repetitive structure of the C_{4v} lattice symmetry. However, the minimum values ($\mathbf{k} = -\mathbf{k}'$) are different: $\zeta^{(h1)}$ nearly reaches -1 , whereas $\zeta^{(h2)} \gtrsim -0.6$ [16]. This reflects the fact that the outer hole band possess a significant overlap with d_{xy} (even) orbitals, while the inner hole band is almost entirely made of odd bands. In a more limited model, where only bands of a certain parity are kept [17], a topological ‘Berry phase winding’

can be defined for each section of the FS [18]. Depending on this ‘winding’, $\zeta_{\mathbf{k},-\mathbf{k}}$ would have to be either +1 or -1; the consequences of the latter would include a suppression of an s -wave VDW in a favor of a p -wave one. Within our model, this notion of topology is absent.

Next, the form factors ζ ’s and γ ’s [16] are used to compute all the interaction vertices (intra, interband and mixed) stemming from (3) along different sections of the FS ($h1$, $h2$, $e1$, and $e2$) and to extract the corresponding coupling constants in the C_4 ‘‘angular momentum’’ channels, s , p , and d . The results, normalized by the overall strength of the screened Coulomb interaction in (3), are

	U				W				G_1	G_2
	(h1)	(h2)	(e1)	(e2)	(h1,e1)	(h1,e2)	(h2,e1)	(h2,e2)	(h1,e1)	(h1,e1)
s	0.44	0.31	0.35	0.35	0.21	0.25	0.27	0.29	0.14	0.14 (9)
p	0.04	0.21	0.17	0.20	0.22	0.21	0.22	0.22	0.01	0.01
d	0.22	0.12	0.09	0.10	0.11	0.13	0.09	0.11	0.03	0.02

Other vertices (G_1, G_2 for either $h2$ or $e2$ bands) are negligibly small in all channels. All the vertices (9) are given in the original c, d electron basis (1-3) and are all positive (repulsive); they are easily converted into the basis used in (5) by the p-h transformation (i.e., $W \rightarrow -W$, etc.).

Obviously, when it comes to the interband vertex (W) as well as all the other vertices, the ‘‘s-wave’’ channel dominates, which retroactively justifies our earlier idealized analysis in terms of a negative U Hubbard model and a fictitious ‘‘superconductor.’’ We find that – depending on the overall strength of Coulomb repulsion – that the most likely ground state is a multiband VDW (SDW/CDW/ODW) which, due to the mismatch of the hole and electron bands and the underlying lattice effects, is generically in the ‘‘FFLO’’ region of the phase digram in Fig. 1, leaving portions of the original FS ungapped and metallic. As expected, this VDW (SDW/CDW/ODW) symmetry breaking at wavevector \mathbf{M} is fueled by a large susceptibility of nearly-nested hole and electron valleys [9].

If the Coulomb repulsion is just below what is needed to produce a metallic VDW (Fig. 1), the mixed ‘‘Josephson’’ vertex G_2 is strongly enhanced, as illustrated by (7) and surrounding discussion. This is the regime where the interband superconductivity [5, 9, 19] is possible. Here, an important point needs to be made: there are *two* ways in which G_2 can lead to high temperature superconductivity in Fe-pnictides: first, G_2 *itself* can be the *source* of superconductivity. This a naturally appealing theoretical scenario, since it relies on the proximity to a SDW instability to enhance G_2 and uses purely electronic interactions to generate superconducting order. The difficulty in this case is that G_2 has to overwhelm the *intra*band Coulomb repulsion U^e and U^h before superconductivity becomes possible, the condition being roughly $G_2 > \sqrt{U^e U^h}$. While G_2 takes off as one approaches the VDW (SDW/CDW/ODW), there is a reflection of this

enhancement in the renormalized values of U^e and U^h as well. For the realistic model with four inequivalent bands and the interaction vertices displayed in Table (9), this balancing act between U ’s and G_2 becomes very sensitive, particularly since the bare U ’s start as generically larger and only $G_2^{(h1,e1)}$ is not negligible in size while all four U s are appreciable. Any effort to extend Eqs. (7) to four bands and to all (intra, interband and mixed) vertices quickly descends into impenetrable numerics with the above sensitivity to the bare values in (9), making it difficult to reach firm conclusions. Some progress along these lines was made in Refs. [19, 20].

The second way is now obvious: G_2 enhancement near the VDW instability can overcome the repulsion U if an *attractive* intraband interaction is at work as well. Such intraband attraction might come from phonons, for example. This attraction itself may or may not suffice to produce superconductivity – the key point is that it reduces the effective U ’s (9) allowing the enhanced G_2 to cross over the hurdle. Note that in both these cases the superconducting gap on the hole and the electron portions of the FS will have the opposite sign [5, 9, 19].

In summary, we have proposed an idealized model of Fe-pnictides which includes an electron and a hole band, and takes advantage of their similar shape and size. The p-h transformation maps this model into a fictitious negative U Hubbard model in external ‘‘Zeeman’’ field. The ground states, fictitious SC and the ‘‘FFLO’’ state, correspond to insulating and metallic VDW in real materials. Next, by considering deviations from perfect nesting, two hole and two electron bands, and other realistic features of Fe-pnictides, we analyze the structure of interactions in the 8+8 orbital model [9] and identify the interband pair resonance mechanism that can generate the *real* superconductivity in the regime where the VDW order gives way to strong VDW fluctuations.

We thank I. Mazin, A. V. Chubukov, M. Kucic, C. Broholm, and W. Bao for useful discussions. This work was supported in part by the NSF grant DMR-0531159.

-
- [1] Y. Kamihara, *et al.*, J. Am. Chem. Soc. **128**, 10012 (2006).
 - [2] Y. Kamihara, *et al.*, J. Am. Chem. Soc. **130**, 3296 (2008).
 - [3] X. H. Chen, *et al.*, Nature **453** 761 (2008); G. F. Chen, *et al.*, Phys. Rev. Lett. **100** 247002 (2008); Z.-A. Ren, *et al.*, Europhys. Lett. **82** 57002 (2008); Mater. Res. Innov. **12**, 105 (2008).
 - [4] S. Lebegue, Phys. Rev. B **75**, 035110 (2007).
 - [5] I. I. Mazin, D. J. Singh, M. D. Johannes, M. H. Du, Phys. Rev. Lett. **101**, 057003 (2008).
 - [6] C. Cao, P. J. Hirschfeld, and H.-P. Cheng, Phys. Rev. B **77**, 220506(R) (2008).
 - [7] R. T. Scalettar, *et al.*, Phys. Rev. Lett. **62**, 1407 (1989); Phys. Rev. Lett. **63**, 218 (1989).
 - [8] K. Kuroki, *et al.*, Phys. Rev. Lett. **101** 087004 (2008).

- [9] V. Cvetkovic, and Z. Tesanovic, arXiv:0804.4678.
- [10] V. Cvetkovic, and Z. Tesanovic, unpublished.
- [11] For properties of FFLO states see H. Shimahara, Phys. Rev. B **62**, 3524 (2000); M. L. Kulić and U. Hofmann, Solid State Comm. **77**, 717 (1991) and references therein.
- [12] A variety of lattice effects in real materials keep the VDW more strongly pinned to \mathbf{M} than in the standard FFLO case [11]. Thus, it is best to identify the “FFLO” state with the metallic VDW (Fig. 1).
- [13] C. de la Cruz, *et al.*, Nature **453**, 899 (2008); Y. Qiu, *et al.*, arXiv:0806.2195.
- [14] D. Bhoi, P. Mandal, and P. Choudhury, arXiv:0807.3833.
- [15] H. Suhl, B. T. Matthias, and L. R. Walker, Phys. Rev. Lett. **3**, 552 (1959).
- [16] <http://www.pha.jhu.edu/~zbt/zetas.html> displays detailed \mathbf{k} -space features of ζ 's and γ 's.
- [17] S. Raghu, X.-L. Qi, C.-X. Liu, D. J. Scalapino, S.-C. Zhang, Phys. Rev. B **77**, 220503(R) (2008).
- [18] Y. Ran, *et al.*, arXiv:0805.3535.
- [19] A. V. Chubukov, D. V. Efremov, I. Eremin, Phys. Rev. B **78**, 134512 (2008).
- [20] F. Wang, *et al.*, arXiv:0805.3343, arXiv:0807.0498.